

# Absorption of ethanol, acetone, benzene and 1,2-dichloroethane through human skin in vitro: a test of diffusion model predictions



Rachna M. Gajjar, Gerald B. Kasting \*

James L. Winkle College of Pharmacy, University of Cincinnati Academic Health Center, Cincinnati, OH 45267-0004, USA

## ARTICLE INFO

### Article history:

Received 30 June 2014

Revised 10 September 2014

Accepted 23 September 2014

Available online 2 October 2014

### Keywords:

Dermal absorption

Percutaneous absorption

Volatile organic compounds

Diffusion model

Evaporation

Skin disposition

## ABSTRACT

The overall goal of this research was to further develop and improve an existing skin diffusion model by experimentally confirming the predicted absorption rates of topically-applied volatile organic compounds (VOCs) based on their physicochemical properties, the skin surface temperature, and the wind velocity. In vitro human skin permeation of two hydrophilic solvents (acetone and ethanol) and two lipophilic solvents (benzene and 1,2-dichloroethane) was studied in Franz cells placed in a fume hood. Four doses of each  $^{14}\text{C}$ -radiolabeled compound were tested – 5, 10, 20, and  $40\ \mu\text{L cm}^{-2}$ , corresponding to specific doses ranging in mass from 5.0 to  $63\ \text{mg cm}^{-2}$ . The maximum percentage of radiolabel absorbed into the receptor solutions for all test conditions was 0.3%. Although the absolute absorption of each solvent increased with dose, percentage absorption decreased. This decrease was consistent with the concept of a stratum corneum deposition region, which traps small amounts of solvent in the upper skin layers, decreasing the evaporation rate. The diffusion model satisfactorily described the cumulative absorption of ethanol; however, values for the other VOCs were underpredicted in a manner related to their ability to disrupt or solubilize skin lipids. In order to more closely describe the permeation data, significant increases in the stratum corneum/water partition coefficients,  $K_{sc}$ , and modest changes to the diffusion coefficients,  $D_{sc}$ , were required. The analysis provided strong evidence for both skin swelling and barrier disruption by VOCs, even by the minute amounts absorbed under these in vitro test conditions.

© 2014 Elsevier Inc. All rights reserved.

## Introduction

The skin is the body's largest organ and first line of defense against harmful exposure. While pharmaceutical companies have sought to overcome the skin barrier in order to deliver therapeutic agents, toxicologists and industrial hygienists have sought to quantify it in order to estimate risk from dermal exposure. With the wide variety of possible permeants physicochemical properties (e.g. polarity, volatility, solubility and molecular weight/volume) and exposure factors (e.g. dose, site and frequency of application, and occlusion) that need to be considered, effective and reliable mathematical models are essential. They can save a great deal of effort compared to experimentally determining absorption rates for the thousands of relevant compounds.

Our laboratory has developed a detailed diffusion model for skin disposition of both volatile and nonvolatile organic compounds with the long-term objective of improving risk assessment for these materials in occupational, environmental and consumer product settings (Dancik et al., 2013). Within the model, special consideration is given

to evaporation of volatile organic compounds (VOCs) from the skin, using a calibration based on in vitro data (Gajjar et al., 2013). In this report, the developed relationships are tested by means of finite dose human skin absorption studies in vitro using two hydrophilic VOCs, ethanol and acetone, and two lipophilic VOCs, benzene and 1,2-dichloroethane (1,2-DCE). We conducted the experiments in a fume hood for safety reasons; however, the associated analysis (Gajjar et al., 2013) allows one to extrapolate the results to other environmental conditions by means of a calibrated mathematical relationship.

Both acetone and ethanol are colorless and highly volatile liquids at room temperature. In cosmetic and personal care products, ethanol is frequently used in the formulation of fragrance, hair care and skin care products and acetone is used in nail polish. In the case of drug products, ethanol functions as an antimicrobial agent and a penetration enhancer. In vitro and in vivo percutaneous absorption studies of neat acetone (Williams et al., 1994) and neat ethanol (Scheuplein and Blank, 1973; Gummer and Maibach, 1986; Pendlington et al., 2001) are rare in the literature. For the case of ethanol, the primary focus has been its ability to enhance the penetration of other compounds when co-administered topically (Berner et al., 1989b).

Benzene has numerous uses, e.g. a constituent in motor fuels; a solvent for fats, waxes, resins, oils, inks, paints, plastics, and rubber; and a solvent for extraction of oils from seeds and nuts. In addition,

\* Corresponding author at: James L. Winkle College of Pharmacy, University of Cincinnati Academic Health Center, P.O. Box 670004, Cincinnati, Ohio 45267-0004, USA. Fax: +1 513 558 0978.

E-mail address: [Gerald.Kasting@uc.edu](mailto:Gerald.Kasting@uc.edu) (G.B. Kasting).

benzene is used in the manufacturing of detergents, explosives, pharmaceuticals, and dyestuffs. The primary uses of 1,2-DCE are as a raw material for the production of vinyl chloride; as a solvent in closed systems for various extractions; cleaning purposes in organic synthesis; a lead scavenger in leaded gasoline; and a dispersant agent for the purpose of wetting and penetrating in rubber and plastics. It is well documented in the literature that individuals employed in industries that manufacture or use benzene maybe exposed to high levels of benzene, which can result in acute and chronic toxicities. For this reason, the EPA has classified benzene as a Group A chemical, i.e. human carcinogen (2009a). However, there is limited epidemiological evidence that 1,2-DCE is a carcinogen, therefore the EPA has classified 1,2-DCE as a Group B2 chemical, i.e. probable human carcinogen (2009c).

Despite serious side effects and warnings, the accurate effects of dermal exposure to benzene and 1,2-DCE are inconclusive due to varying experimental conditions. In vitro and in vivo percutaneous absorption studies of neat benzene (Laserew et al., 1931; Ceasaro, 1946; Conca and Maltagliati, 1955; Hanke et al., 1961; Maibach and Anjo, 1981; Tsuruta, 1982; Franz, 1984; Susten et al., 1985; Lodén, 1986; Morgan et al., 1991) are extensive in the literature. This work and related animal dermal absorption studies have been summarized and analyzed in an excellent review (Williams et al., 2011). Literature data for neat 1,2-dichloroethane are more limited (Ceasaro, 1946; Tsuruta, 1989; Morgan et al., 1991; Frasch et al., 2007); Frasch et al.'s (2007) results are discussed later in this report.

To the best of our knowledge there is no standardized methodology for estimating absorption from small doses of liquid VOCs that are splashed on the skin. The goal of this study is to present one possible methodology and to determine how effectively the results can be predicted from physiochemical properties and exposure conditions using the current skin absorption model (Dancik et al., 2013).

## Materials and methods

### Chemicals

$^{14}\text{C}$ -Ethanol at specific activity 2.8 mCi/mmol and  $^{14}\text{C}$ -benzene at specific activity 15.6 mCi/mmol were purchased from Sigma-Aldrich (St. Louis, MO).  $^{14}\text{C}$ -Acetone at specific activity 20 mCi/mmol and  $^{14}\text{C}$ -1,2-DCE at specific activity 5.0 mCi/mmol were purchased from American Radiolabeled Chemicals (St. Louis, MO). Radiochemical purities as stated by both suppliers were 100%, 99.3%, 100% and 99.0%, respectively. Unlabeled neat ethanol was purchased from Aaper (Shelbyville, KY) and unlabeled neat acetone was purchased from J.T. Baker (Phillipsburg, NJ). Unlabeled neat benzene, 1,2-DCE and calcium-free Dulbecco's phosphate-buffered saline were purchased from Sigma-Aldrich (St. Louis, MO). Ultima Gold® Scintillation fluid and Soluene-350™ were purchased from PerkinElmer Biosciences. Sodium azide was purchased from Fisher Scientific (Pittsburgh, PA). All other chemicals used were reagent grade.

### Finite dose solvent absorption

Tissue preparation and handling have been previously described (Kasting and Bowman, 1990; Kasting et al., 1994). Dermatomed split thickness human cadaver skin (~0.3 mm), either from the back, abdomen or thigh, treated with 10% glycerol solution and stored in the foil packs at  $-80\text{ }^{\circ}\text{C}$  was obtained from U.S. Tissue and Cell or the New York Fire Fighter Skin Bank (New York, NY). Prior to conducting an in vitro percutaneous absorption study, the skin was gently thawed in  $35\text{--}40\text{ }^{\circ}\text{C}$  distilled water and then rinsed with either distilled water or Dulbecco's phosphate-buffered saline, pH 7.4, preserved with 0.02% sodium azide (PBS) to remove any glycerol used in the preservation process. The skin was cut into  $\sim 1.5\text{ cm} \times 1.5\text{ cm}$  squares using a 22 blade scalpel and mounted onto modified Franz diffusion cells ( $0.79\text{ cm}^2$ ) with the stratum corneum facing the donor compartment

and the dermis contacting the receptor compartment. Non-occluded glass tops, which were open to the atmosphere and extended 4 mm above the skin surface, were placed on top of the cells and firmly clamped in place. The receptor compartments were filled with PBS, taking care to remove any air bubbles trapped between the skin and receptor solution. The cells were then placed into aluminum blocks, which were placed in a Pierce Reacti-Therm 18900 Heating and Stirring Module (Rockford, IL). Micromagnetic stir bars were placed into the receptor compartments of the cells to ensure stirring throughout the experiment. The aluminum blocks were maintained at  $37 \pm 2\text{ }^{\circ}\text{C}$ , resulting in a stratum corneum temperature of  $32 \pm 2\text{ }^{\circ}\text{C}$ . In order to keep radiochemicals out of the laboratory atmosphere, the modules were placed in a fume hood with the sash height at 18 in. This arrangement mimicked outdoor wind conditions (Ray Chaudhuri et al., 2009).

After equilibrating the mounted skin for 2 h in the diffusion cell, a tissue integrity test was performed using  $^3\text{H}_2\text{O}$ . The specifics of the test are described in detail elsewhere (Franz and Lehman, 1990; Kasting et al., 1994); briefly, the procedure was as follows. The tissue was screened by exposing each mounted  $0.79\text{ cm}^2$  skin piece to  $150\text{ }\mu\text{L}$  of tritiated water ( $0.4\text{ }\mu\text{Ci/mL}$ ) for 5 min, followed by gentle removal the dose using one cotton tip applicator. At 60 min post dose, the receptor fluid was collected in 12 mL of Ultima® Gold Scintillation Fluid (PerkinElmer Inc., Wellesley, MA) and analyzed by Beckman LS 6500 TM scintillation counter (Beckman Coulter Inc., Fullerton, CA). Based on  $^3\text{H}_2\text{O}$  permeation results, samples with water permeation values greater than  $1.2\text{ }\mu\text{L/cm}^2$  were discarded. The remaining samples were then randomized over treatments. Following the test, the receptor solution was exchanged twice to ensure complete removal of residual radioactivity. The skin samples were then allowed to equilibrate overnight.

The doses of  $^{14}\text{C}$ -ethanol were 5, 10, 20 and  $40\text{ }\mu\text{L}$  per  $0.79\text{ cm}^2$  cell with specific activity of  $0.35\text{ }\mu\text{Ci}/\mu\text{L}$ , yielding a dose of 5.0, 10.0, 20.0 and  $40.0\text{ mg cm}^{-2}$ , respectively, and the doses of  $^{14}\text{C}$ -acetone were 5, 10, 20 and  $40\text{ }\mu\text{L}$  per  $0.79\text{ cm}^2$  cell with specific activity of  $0.05\text{ }\mu\text{Ci}/\mu\text{L}$ , yielding a dose of 5.0, 9.9, 19.9 and  $39.7\text{ mg cm}^{-2}$ , respectively. The doses of  $^{14}\text{C}$ -benzene were 5, 10, 20 and  $40\text{ }\mu\text{L}$  per  $0.79\text{ cm}^2$  with specific activity of  $0.05\text{ }\mu\text{Ci}/\mu\text{L}$ , yielding a dose of 5.5, 11.1, 22.2 and  $44.4\text{ mg cm}^{-2}$  and the doses of  $^{14}\text{C}$ -1,2-DCE were 5, 10, 20 and  $40\text{ }\mu\text{L}$  per  $0.79\text{ cm}^2$  cell, with specific activity of  $0.05\text{ }\mu\text{Ci}/\mu\text{L}$ , yielding a dose of 7.9, 15.8, 31.5 and  $63.1\text{ mg cm}^{-2}$ , respectively. The receptor solutions were collected and refilled at predetermined time points: 5, 10, 15, 20, 40 min and 1, 2, 4, 8, 24 h post-dose. To minimize the loss of the permeant from the receptor solution, the collected receptor solution was poured immediately into a scintillation vials prefilled with 12 mL of scintillation fluid. Within 1 h of collecting the receptor solution, the vials were measured for radioactivity by liquid scintillation counting (LSC). Following the last receptor collection, the skin samples were removed from the diffusion cells, dissolved in 2 mL of Soluene overnight at room temperature, and analyzed by LSC. Permeation was measured on the skin from three donors, with  $n = 2\text{--}7$  per donor per dose. Most conditions were tested with 4–5 replicates  $\times$  3 donors, yielding a total  $n$  value of 12–15 per dose condition. All data were first averaged by dose for each donor and then averaged across donors to obtain the reported results.

## Data analysis

### Physical properties

Physical properties of ethanol, acetone, benzene and 1,2-DCE relevant to skin absorption were obtained from the EpiSuite program available from the U.S. Environmental Protection Agency (US\_EPA, 2009b) unless otherwise noted (Table 1).

### Diffusion model

The disposition of ethanol, acetone, benzene and 1,2-DCE in the finite dose solvent absorption study was estimated using the current

**Table 1**  
Physical properties of ethanol, acetone, benzene and 1,2-DCE.<sup>a</sup>

Property	Units	Value			
		Ethanol	Acetone	Benzene	1,2-DCE
MW	g mol <sup>-1</sup>	46	58	78	99
$\rho^b$	g cm <sup>-3</sup>	0.78	0.78	0.86	1.23
$\log K_{\text{oct}}^c$	–	–0.31	–0.24	2.13	1.48
$P_{\text{vp}}^d$	torr	84	301	129	110
$S_w^e$	g L <sup>-1</sup>	779	776	1.79 <sup>f</sup>	8.6 <sup>g</sup>

<sup>a</sup> All properties are estimated at 32 °C values. Properties were obtained from (US EPA, 2009b) unless otherwise noted and extrapolated to 32 °C as required.

<sup>b</sup> Density.

<sup>c</sup> Octanol/water partition coefficient.

<sup>d</sup> Vapor pressure.

<sup>e</sup> Water solubility.

<sup>f</sup> Extrapolated from measured value of 1.79 g/L at 25 °C.

<sup>g</sup> Extrapolated from measured value of 8.6 g/L at 25 °C.

diffusion/evaporation model (Kasting et al., 2008a; Dancik et al., 2013). The diffusion/evaporation model is a one-dimensional model including three skin layers – the stratum corneum ( $i = \text{sc}$ ), viable epidermis ( $i = \text{ed}$ ) and dermis ( $i = \text{de}$ ). Each layer has a representative thickness ( $h_i$ ), diffusivity ( $D_i$ ) and partition coefficient with respect to water ( $K_i$ ); in addition, there is a first-order clearance constant ( $k_{\text{de}}$ ) in the dermis representing systemic absorption by the skin capillaries. The most recent description of the model may be found in Dancik et al. (2013), and we refer the reader to this article for details. The calculation is freely available from the authors in Excel® spreadsheet form and may furthermore be accessed on the NIOSH/CDC website as the Finite Dose Skin Permeation Calculator (Fedorowicz et al., 2011). The studies in this research involve hydrophilic to moderately lipophilic liquids ( $\log K_{\text{oct/w}} \leq 3$ ) for which the resistance of the viable tissue layers is low compared to SC. Hence, the primary focus is on SC properties.

In order to compare the a priori calculation to the experimental data, two calculations were performed. First, to determine the diffusion model prediction parameters, the physical properties listed in Table 1 for ethanol, acetone, benzene and 1,2-DCE were used to estimate transport parameters for the predictive calculation (Kasting et al., 2008a; Dancik et al., 2013). The effective air flow velocity in the evaporative mass transfer correlation for hood studies was revised to 0.92 m s<sup>-1</sup> as a result of volatile organic solvent evaporation studies (Gajjar et al., 2013).

Second, to determine the fitted model parameters, a calculation was conducted in which the diffusion and partition coefficients in the stratum corneum of the volatile organic solvent were modified to fit the experimental data. The parameters were fitted to the data using a nonlinear least squares fitting (Santhanam et al., 2005; Miller et al., 2006) routine adapted from Bevington (Bevington, 1969). The code was implemented as a Visual Basic® add-in for Microsoft Excel®. Quality of fit was assessed by comparing the sum of squared residuals, normalized by degrees of freedom as defined by Bevington

$$\chi^2_{\nu} = \frac{1}{n-p} \sum_{i=1}^n [y_i(\text{obs}) - y_i(\text{fit})]^2 \quad (1)$$

where  $n$  was the number of observations,  $p$  the number of adjustable parameters, and the  $y_i$  values were cumulative percents of dose permeated at the specified sampling times. In this scenario the effective evaporation rate constant  $k_{\text{evap}}$  was fixed to the experimentally measured value listed in Table 3.

From this point forward, the parameters associated with the two calculations will be referred to as “a priori” and “fitted” parameters, respectively.

## Results

The mean cumulative amount radioactivity permeated associated with <sup>14</sup>C-ethanol, <sup>14</sup>C-acetone, <sup>14</sup>C-benzene and <sup>14</sup>C-1,2-DCE over 24 h

as a function of time and applied dose is shown in Table 2. Representative plots of the mean percentage of radioactive dose permeated over 24 h as functions of time and applied dose are shown in Fig. 1. It is evident from these results that the majority of the applied <sup>14</sup>C-ethanol, <sup>14</sup>C-acetone, <sup>14</sup>C-benzene and <sup>14</sup>C-1,2-DCE dose evaporated from the skin's surface during the study.

With one exception, a consistent pattern of increasing permeation with decreasing dose and hence, decreasing percent absorption with increasing dose for the 40, 20, 10 and 5 mg cm<sup>-2</sup> data was seen. However, the permeation results for the 10 mg cm<sup>-2</sup> ethanol dose were higher than those of 5 mg cm<sup>-2</sup>. This was a result of the mean values for the former being skewed by high absorption in a few individual diffusion cells rather than an overall higher permeation rate. The 10 mg cm<sup>-2</sup> ethanol data were consequently excluded from the dataset used to fit the diffusion model parameters.

Flux profiles for the lowest dose of each VOC tested are shown in Fig. 2 along with the two model calculations. The symbols represent the experimental flux plotted as the midpoint of the collection interval. Maximum absorption rates were reached within 10–20 min post-dose for each VOC. The dashed curve represents the diffusion model prediction using the a priori parameter values in Table 3. The solid line represents the fitted model calculation using the diffusion coefficient ( $D_{\text{sc}}$ ), partition coefficient ( $K_{\text{sc}}$ ) and evaporative mass transfer coefficient ( $k_{\text{evap}}$ ) correction factors given in Table 3.

### <sup>14</sup>C-Ethanol

The cumulative percent of dose absorbed over 24 h ranged from 0.25% (12.6 µg cm<sup>-2</sup>) for the 5.0 mg cm<sup>-2</sup> dose to 0.17% (66.3 µg cm<sup>-2</sup>) for the 40.0 mg cm<sup>-2</sup> dose (Fig. 1). The amount of radioactivity remaining in the tissue 24 h after application was less than 0.07% (data not shown).

For the 5.0 mg cm<sup>-2</sup> applied <sup>14</sup>C-ethanol dose, the a priori calculation overestimated the initial permeation rate through the skin, but slightly underestimated total permeation (Fig. 2a). The latter was underpredicted by a factor of 1.3. Improvement to the a priori model calculations was obtained by adjusting the ethanol diffusion and partition coefficients in the stratum corneum, as represented by the solid line in the figure. The multiplicative correction factors for the stratum corneum diffusion and partition coefficient obtained by simultaneously fitting the two parameters over all doses were 0.27 for diffusivity and 3.00 for partition coefficient, with an  $r^2$  value of 0.97 (Table 3).

### <sup>14</sup>C-Acetone

The cumulative percent of dose absorbed over 24 h ranged from 0.3% (15.2 µg cm<sup>-2</sup>) at 4.9 mg cm<sup>-2</sup> dose to 0.15% (58.9 µg cm<sup>-2</sup>) at 39.7 mg cm<sup>-2</sup> dose (Fig. 1). The amount of radioactivity remaining in the tissue 24 h after application was less than 0.03% (data not shown).

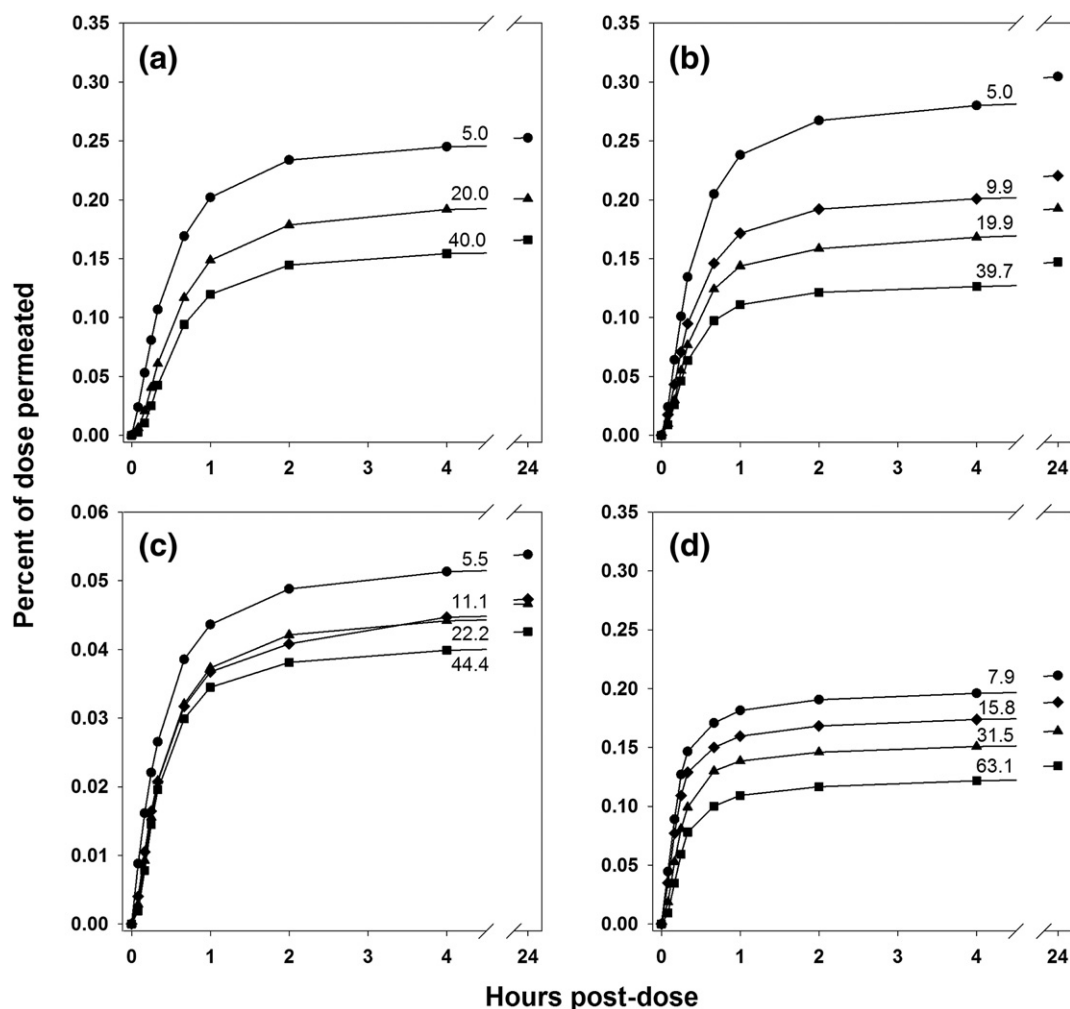
For the 5.0 mg cm<sup>-2</sup> applied <sup>14</sup>C-acetone dose, the a priori calculation accurately estimated the initial permeation rate, but significantly underestimated total permeation through the skin by a factor of 4.7 (Fig. 2b). As with ethanol, improvement to the a priori model calculations was achieved by adjusting the diffusion and partition coefficients in the stratum corneum, as represented by the solid line in the figure. Least-squares estimates of the multiplicative correction factors for these parameters were 0.5 for diffusivity and 5.29 for partition coefficient, with an  $r^2$  value of 0.91 (Table 3).

### <sup>14</sup>C-Benzene

The cumulative percent of dose absorbed over 24 h ranged from 0.5% (3.0 µg cm<sup>-2</sup>) at the 5.5 mg cm<sup>-2</sup> dose to 0.04% (9.0 µg cm<sup>-2</sup>) at the 44.4 mg cm<sup>-2</sup> dose. The amount of radioactivity remaining in the tissue 24 h after application was less than 0.03% (data not shown).

**Table 2**Permeation of VOCs through human skin in vitro (mean  $\pm$  SE of three donors, n = 2–7 cells per donor).

Dose (mg cm <sup>-2</sup> )	Cumulative amount permeated ( $\mu$ g cm <sup>-2</sup> )									
	5 min	10 min	15 min	20 min	40 min	60 min	2 h	4 h	8 h	24 h
<b><sup>14</sup>C-Ethanol</b>										
5.0	1.2 $\pm$ 0.4	2.6 $\pm$ 0.8	4.0 $\pm$ 1.1	5.3 $\pm$ 1.5	8.4 $\pm$ 3.5	10.1 $\pm$ 4.8	11.7 $\pm$ 6.4	12.2 $\pm$ 6.8	12.5 $\pm$ 7.0	12.6 $\pm$ 7.0
10.0 <sup>a</sup>	1.7 $\pm$ 0.6	6.2 $\pm$ 2.0	11.5 $\pm$ 3.4	15.6 $\pm$ 4.4	26.8 $\pm$ 6.8	32.3 $\pm$ 8.1	36.7 $\pm$ 9.2	38.3 $\pm$ 9.6	39.0 $\pm$ 9.6	39.5 $\pm$ 9.6
20.0	1.2 $\pm$ 0.3	4.1 $\pm$ 1.0	8.1 $\pm$ 1.1	12.2 $\pm$ 1.5	23.3 $\pm$ 7.2	29.7 $\pm$ 11.9	35.7 $\pm$ 17.4	38.3 $\pm$ 20.1	39.4 $\pm$ 20.9	40.1 $\pm$ 21.1
40.0	1.1 $\pm$ 0.2	4.3 $\pm$ 1.0	10.0 $\pm$ 1.3	17.0 $\pm$ 0.8	37.6 $\pm$ 7.5	47.8 $\pm$ 13.2	57.8 $\pm$ 19.3	61.6 $\pm$ 21.8	63.4 $\pm$ 22.5	66.3 $\pm$ 22.8
<b><sup>14</sup>C-Acetone</b>										
5.0	1.2 $\pm$ 0.4	3.2 $\pm$ 1.1	5.0 $\pm$ 1.7	6.7 $\pm$ 2.4	10.2 $\pm$ 3.9	11.9 $\pm$ 4.6	13.4 $\pm$ 5.1	14.0 $\pm$ 5.1	14.5 $\pm$ 5.1	15.2 $\pm$ 5.2
9.9	1.8 $\pm$ 0.2	4.3 $\pm$ 1.1	7.1 $\pm$ 2.4	9.5 $\pm$ 3.5	14.6 $\pm$ 6.1	17.2 $\pm$ 7.2	19.2 $\pm$ 8.0	20.1 $\pm$ 8.2	20.8 $\pm$ 8.1	22.1 $\pm$ 8.2
19.9	1.9 $\pm$ 0.3	5.9 $\pm$ 1.6	11.0 $\pm$ 3	15.3 $\pm$ 4.1	24.8 $\pm$ 5.8	28.8 $\pm$ 6.7	31.7 $\pm$ 7.3	33.6 $\pm$ 7.6	35.5 $\pm$ 7.7	38.5 $\pm$ 8.2
39.7	3.6 $\pm$ 2.0	10.4 $\pm$ 5.4	18.5 $\pm$ 8.5	25.4 $\pm$ 10.7	38.9 $\pm$ 13.7	44.4 $\pm$ 14.6	48.6 $\pm$ 15.2	50.5 $\pm$ 15.4	52.9 $\pm$ 15.3	58.9 $\pm$ 16.0
<b><sup>14</sup>C-Benzene</b>										
5.5	0.49 $\pm$ 0.13	0.90 $\pm$ 0.08	1.23 $\pm$ 0.11	1.48 $\pm$ 0.12	2.15 $\pm$ 0.14	2.43 $\pm$ 0.02	2.72 $\pm$ 0.05	2.86 $\pm$ 0.05	2.93 $\pm$ 0.07	3.00 $\pm$ 0.10
11.1	0.45 $\pm$ 0.05	1.17 $\pm$ 0.12	1.83 $\pm$ 0.22	2.31 $\pm$ 0.30	3.53 $\pm$ 0.41	4.09 $\pm$ 0.42	4.55 $\pm$ 0.46	4.98 $\pm$ 0.40	5.12 $\pm$ 0.39	5.27 $\pm$ 0.38
22.2	0.64 $\pm$ 0.20	2.06 $\pm$ 0.65	3.46 $\pm$ 0.83	4.65 $\pm$ 1.03	7.14 $\pm$ 0.97	8.31 $\pm$ 0.84	9.38 $\pm$ 0.68	9.84 $\pm$ 0.58	10.09 $\pm$ 0.56	10.39 $\pm$ 0.46
44.4	0.85 $\pm$ 0.28	3.48 $\pm$ 1.41	6.47 $\pm$ 2.34	8.72 $\pm$ 2.90	13.32 $\pm$ 3.70	15.36 $\pm$ 3.88	16.97 $\pm$ 3.95	17.76 $\pm$ 3.97	18.31 $\pm$ 3.97	18.98 $\pm$ 4.05
<b><sup>14</sup>C-1,2-DCE</b>										
7.9	2.9 $\pm$ 0.4	5.9 $\pm$ 0.9	8.5 $\pm$ 1.5	9.9 $\pm$ 2.1	11.5 $\pm$ 2.5	12.3 $\pm$ 2.8	12.9 $\pm$ 3.0	13.2 $\pm$ 3.1	13.6 $\pm$ 3.0	14.2 $\pm$ 2.9
15.8	5.5 $\pm$ 1.5	12.1 $\pm$ 2.0	17.1 $\pm$ 3.7	20.2 $\pm$ 4.9	23.5 $\pm$ 6.3	25.0 $\pm$ 6.9	26.4 $\pm$ 7.5	27.3 $\pm$ 7.7	28.1 $\pm$ 7.7	29.6 $\pm$ 7.6
31.5	5.9 $\pm$ 0.8	16.6 $\pm$ 1.0	25.4 $\pm$ 3.0	31.1 $\pm$ 4.5	40.8 $\pm$ 7.6	43.5 $\pm$ 7.9	45.8 $\pm$ 8.2	47.3 $\pm$ 8.3	48.8 $\pm$ 8.2	51.4 $\pm$ 8.1
63.1	5.8 $\pm$ 1.6	21.9 $\pm$ 2.4	37.2 $\pm$ 3.3	49.0 $\pm$ 6.5	62.8 $\pm$ 9.4	68.6 $\pm$ 11.1	73.2 $\pm$ 12.2	76.4 $\pm$ 12.2	79.3 $\pm$ 11.9	84.4 $\pm$ 11.4

<sup>a</sup> Excluded from analysis as explained in the text.**Fig. 1.** Percentage of radioactive dose associated with (a) <sup>14</sup>C-ethanol, (b) <sup>14</sup>C-acetone, (c) <sup>14</sup>C-benzene and (d) <sup>14</sup>C-1,2-DCE permeation in the receptor solution following application to human skin in vitro (mean  $\pm$  SE of three donors, n = 2–7 cells per donor). The numbers on the graph are the applied dose of VOC in mg cm<sup>-2</sup>.



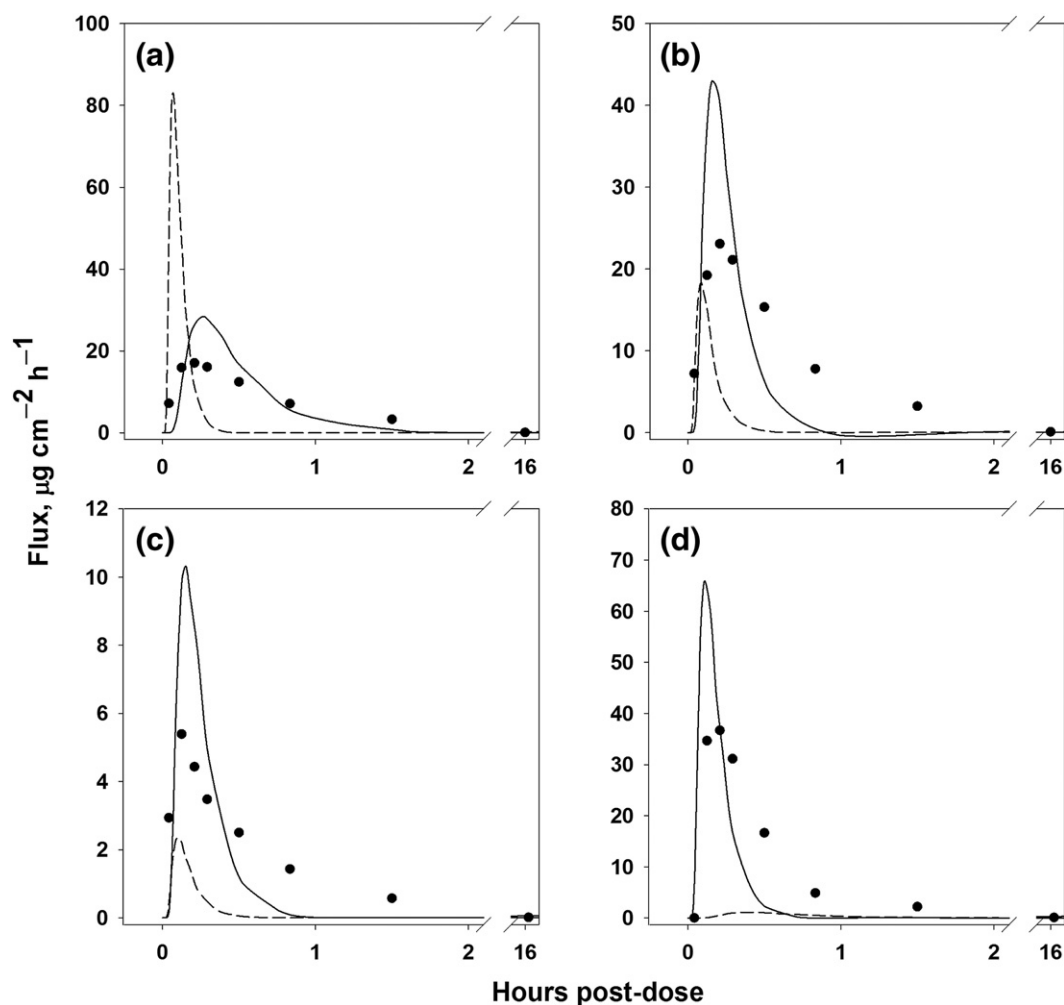


**Fig. 2.** Flux of VOC into the receptor solution following application of VOC to human skin in vitro (mean  $\pm$  SE of three donors,  $n = 2$ –7 cells per donor) (a)  $^{14}\text{C}$ -ethanol;  $5.0 \text{ mg cm}^{-2}$ , (b)  $^{14}\text{C}$ -acetone;  $5.0 \text{ mg cm}^{-2}$ , (c)  $^{14}\text{C}$ -benzene;  $5.5 \text{ mg cm}^{-2}$  and (d)  $^{14}\text{C}$ -1,2-DCE;  $7.9 \text{ mg cm}^{-2}$ . Symbols—experimental flux plotted as the midpoint of the collection interval; dashed line—a priori flux calculations using the parameters in Table 3; and solid line—fitted flux calculations using the parameters associated with the fit of the model to the displayed dose data only.

For the  $5.5 \text{ mg cm}^{-2}$  dose, the a priori calculation significantly underestimated both the initial skin permeation rate of  $^{12}\text{C}$ -benzene and the total permeation (Fig. 1c). The latter was underpredicted by a factor of 6.5. Considerable improvement to the a priori model calculations was obtained by adjusting the diffusion and partition coefficients in the

stratum corneum, as represented by the solid line in the figure. The multiplicative correction factors for these parameters were 0.68 for diffusivity and 8.00 for partition coefficient, with an  $r^2$  value of 0.78 (Table 3).

#### $^{14}\text{C}$ -1,2-DCE

The cumulative percent of dose absorbed over 24 h ranged from 0.21% ( $14.2 \text{ μg cm}^{-2}$ ) for the  $7.9 \text{ mg cm}^{-2}$  dose to 0.13% ( $84.4 \text{ μg cm}^{-2}$ ) for the  $63.1 \text{ mg cm}^{-2}$  dose. The amount of radioactivity remaining in the tissue 24 h after application was less than 0.08% (data not shown).

For the  $7.9 \text{ mg cm}^{-2}$  applied  $^{12}\text{C}$ -1,2-DCE dose, the a priori calculation severely underestimated both the initial permeation rate and the total permeation through the skin (Fig. 2d). The latter was underpredicted by a factor of 15.9. Improvement to the a priori model calculations was obtained by adjusting the  $^{12}\text{C}$ -1,2-DCE diffusion and partition coefficients in the stratum corneum, as represented by the solid line in the figure. The multiplicative correction factors for these parameters were 3.7 for diffusivity and 9.0 for partition coefficient, with an  $r^2$  value of 0.88 (Table 3).

## Discussion

### Comparison of present studies with previously published permeation studies

Ethanol is the solvent for three well known transdermal therapeutic systems: estradiol (Campbell and Chandrasekaran, 1983; Good et al.,

**Table 3**  
Parameters of a priori diffusion model to fitted/experimental values of  $^{14}\text{C}$ -ethanol,  $^{14}\text{C}$ -acetone,  $^{14}\text{C}$ -benzene and  $^{14}\text{C}$ -1,2-DCE in the receptor solutions.

Parameters	Units	Values			
		Ethanol	Acetone	Benzene	1,2-DCE
<i>A priori model values<sup>a</sup></i>					
$D_{\text{SC}} \times 10^{10}$	$\text{cm}^2 \text{ s}^{-1}$	6.78	4.60	4.08	1.01
$K_{\text{SC}}$	–	0.39	0.39	17.74	11.17
$k_{\text{evap}} \times 10^3$	$\text{cm s}^{-1}$	0.12	0.50	0.19	0.16
<i>Fitted/experimental values expressed as a multiple of a priori value</i>					
$D_{\text{SC}}^{\text{b}}$	–	0.27	0.50	0.68	3.70
$K_{\text{SC}}^{\text{b}}$	–	3.00	5.29	8.06	9.00
$k_{\text{evap}}^{\text{c}}$	–	0.98	1.13	1.00	0.98
<i>Statistics</i>					
$n$	–	10	10	10	10
$s$	% dose	0.020	0.025	0.007	0.018
$r^2$	–	0.97	0.91	0.78	0.88

<sup>a</sup> (Dancik et al., 2013).

<sup>b</sup> Least squares values.

<sup>c</sup> Experimental values.

1985), nitroglycerin (Gale and Berggen, 1987) and fentanyl (Gale et al., 1984). Three key features of ethanol as a skin penetration enhancer are the linearity of drug transport with ethanol transport across skin (Campbell and Chandrasekaran, 1983; Good et al., 1985), a maximum ethanol flux across skin of  $1300 \mu\text{g cm}^{-2} \text{h}^{-1}$  (Berner et al., 1989a) and, possibly, a 5–10 fold increases in drug flux across skin when administered as a co-solvent with water (Berner et al., 1989b).

An additional advantage of utilizing ethanol for enhancement of drug flux is the low degree of irreversible barrier disruption. Ethanol has been shown to moderately disrupt stratum corneum intercellular lipids, however these changes were reversed within 24 h post exposure (Bommanna et al., 1991). Acetone, on the other hand, extracts sizable amounts of surface lipids (triglycerides, wax, esters, squalene, cholesterol esters) relative to water, however, it proves to be a poor barrier disrupter after 12 min of topical exposure (Abrams et al., 1993). It has been used extensively as a barrier perturbation tool in mouse (Man et al., 1993; Denda et al., 1996), yet Fatasch showed no morphological changes in human skin following 1 and 3 h application of acetone, only after 5 h of exposure was an enhancement in transepidermal water loss, visible intercellular disruption, loss of cohesion between the layers detected (Fatasch, 1997). One could say it is a mild barrier disrupter.

For ethanol, the maximum flux was reached within 10–20 min post-dose for all doses tested, with values ranging from  $17.5$  to  $83.5 \mu\text{g cm}^{-2} \text{h}^{-1}$ . The cumulative amount permeated through human cadaver skin ranged from  $12.6 \mu\text{g cm}^{-2}$  (0.25%) for the  $4.9 \text{ mg cm}^{-2}$  dose to  $66.3 \mu\text{g cm}^{-2}$  (0.17%) for the  $40.0 \text{ mg cm}^{-2}$  dose. These values are considerably lower than other published values. For example, Pendlington showed ethanol penetration through pig skin in vitro to be  $0.10 \text{ mg cm}^{-2}$  (2.0% of dose) for a  $4.9 \text{ mg cm}^{-2}$  dose in 24 h (Pendlington et al., 2001). Likewise, Gummer et al. demonstrated the total amount of ethanol that permeated guinea-pig skin in vitro over a period of 19 h was in the order of 1% of the total dose (Gummer and Maibach, 1986) and Williams et al. showed that 95% of the ethanol evaporated in the first 2 min after dosing, with less than 3% left after 2 h in IPPSF chamber experiments (Williams et al., 1994). It is important to note that the cited studies were conducted at ambient conditions without occlusion. The airflow was thus less than that in our studies, where the fume hood generated an average wind velocity of  $0.92 \text{ m s}^{-1}$  above the modified Franz diffusion cells (Gajjar et al., 2013). The increased airflow in the present study resulted in increased evaporation rate of ethanol and consequently lower permeation.

The acetone data presented herein show that the majority of the dose evaporated from the skin's surface. Our results do not accord with the published acetone permeation study Williams et al. (Williams et al., 1994). Using the isolated perfused porcine skin flap (IPPSF) method, these investigators found that 60% of the dosed acetone evaporated in the first 2 min, with 33% remaining after 2 h. Our in vitro human cadaver skin permeation study showed cumulative absorption values ranging from  $15.2 \mu\text{g cm}^{-2}$  (0.3%) for the  $4.9 \text{ mg cm}^{-2}$  dose to  $58.9 \mu\text{g cm}^{-2}$  (0.15%) for the  $39.7 \text{ mg cm}^{-2}$  dose. Maximum flux was reached within the 15 min post-dose for all doses tested. The values ranged from  $24.0$  to  $97.6 \mu\text{g cm}^{-2} \text{h}^{-1}$ , with little to no flux after about 2 h. Thus, we found acetone evaporation and permeation to be rapid, similar to that of ethanol.

Benzene is a common gasoline additive and is also used in the production of drugs, dyes, detergents, rubbers, and pesticides. Over the past six decades, many studies have been conducted to assess the extent of absorption of benzene in animals and humans; this work has been excellently summarized by Williams et al. (2011). Studies assessing 1,2-DCE are considerably less frequent (Tsuruta, 1975; Tsuruta, 1977; Morgan et al., 1991; Frasch et al., 2007). However 1,2-DCE is of similar importance to benzene in terms of exposure because it is widely used in the production of polyvinyl chloride, the third most-widely produced polymer.

Our results for benzene show that the majority of the applied dose evaporated from the skin's surface during the study. This conclusion is in line with other published results (Williams et al., 2011). However, a major distinction between our in vitro human cadaver skin permeation studies and others is that our studies were conducted in the fume hood, whereas the other studies were conducted under ambient conditions. We found cumulative absorption values for benzene ranging from  $3.0 \mu\text{g cm}^{-2}$  (0.05%) for the  $5.5 \text{ mg cm}^{-2}$  dose to  $9.0 \mu\text{g cm}^{-2}$  (0.04%) for the  $44.4 \text{ mg cm}^{-2}$  dose. Maximum flux was reached within 5–20 min post-dose for all doses tested and ranged from  $5.9$ – $35.8 \mu\text{g cm}^{-2} \text{h}^{-1}$ . It is noteworthy that the specific doses in our study were lower than several of those listed in Williams et al. (2011) and the percentages of dose permeated were smaller. This difference reflects the higher airflow in our study.

The 1,2-DCE data show that the maximum flux was reached within 10 min post-dose for all doses tested, with values ranging from  $37$  to  $193 \mu\text{g cm}^{-2} \text{h}^{-1}$ . The cumulative absorbed amount ranged from  $14.2 \mu\text{g cm}^{-2}$  (0.21%) for the  $7.9 \text{ mg cm}^{-2}$  dose to  $84.4 \mu\text{g cm}^{-2}$  (0.13%) for  $63.1 \text{ mg cm}^{-2}$  dose. The majority of the applied dose evaporated from the skin's surface. This conclusion is in line with other published results; however, our data showed higher evaporation, consistent with the fume hood environment (Tsuruta, 1975; Tsuruta, 1977; Morgan et al., 1991). Also, the species, site and experimental method differed significantly from the cited studies.

#### Comparison of present studies with diffusion/evaporation model

The most important assumption of our computational model (Kasting et al., 2008b; Nitsche and Kasting, 2008; Dancik et al., 2013), which is available to toxicologists as the Finite Dose Skin Permeation Calculator on the NIOSH/CDC website (Fedorowicz et al., 2011), is that the absorption and evaporation of a volatile organic compound on the skin can be estimated from the physical properties listed in Table 1 and the environmental factors temperature ( $T$ ) and wind velocity ( $u$ ). In the present studies the latter factors were  $32^\circ\text{C}$  and  $0.92 \text{ m s}^{-1}$ , respectively. However, calibrated relationships for both temperature (Kasting et al., 2008b) and wind velocity (Gajjar et al., 2013) are incorporated into the model, allowing predictions to be made for a variety of conditions. Absorption parameters, such as, diffusivities ( $D_i$ ) and partition coefficients ( $K_i$ ) for each skin layer are calculated from the physical properties listed in Table 1. The  $K_i$  value for the stratum corneum is utilized to obtain the saturation concentration of the solvent in this layer ( $C_{\text{sat}}$ ) and the amount of the chemical required to saturate the deposition region ( $M_{\text{sat}}$ ). The deposition region, thickness  $h_{\text{dep}}$ , is the upper part of the stratum corneum into which topically applied chemicals rapidly penetrate (Kasting and Miller, 2006). The ratio of the applied dose ( $M_0$ ) to  $M_{\text{sat}}$  distinguishes a small dose ( $M_0/M_{\text{sat}} < 1$ ) from a large dose ( $M_0/M_{\text{sat}} > 1$ ). Transient disposition on the skin is a function of this ratio combined with the dimensionless volatility parameter ( $\chi$ ). Higher values of  $\chi$  favor evaporation over absorption. The equations for the abovementioned transport parameters are given in detail in Dancik et al. (2013) and derive from a considerable body of research (cf. references in Dancik et al., 2013). In the case of the four solvents studied herein, the applied doses led to similar absorption profiles despite the difference in the doses. This result may be explained by the fact that the ratios of  $M_0/M_{\text{sat}}$  were greater than 1; thus all the doses were large.

The analysis shows discrepancies between the a priori model and the experimental data (Table 3). Four key parameters – evaporation rate, deposition region, diffusion and partition coefficients – are analyzed below in order to better understand the sources of error.

#### Evaporation rates

For all VOCs the evaporation rate constants,  $k_{\text{evap}}$ , calculated using the predetermined wind velocity of  $0.92 \text{ m s}^{-1}$  (Gajjar et al., 2013)

matched those determined by least squares fitting to the experimental data to within 13% (Table 3). These differences were within the root mean square error of 20% in the original velocity determinations (Gajjar et al., 2013). Thus the a priori model predictions satisfactorily described the experimental data and the 95% confidence interval limits provided no addition evidence to re-evaluate the predetermined wind velocity.

### Deposition region

The deposition region, thickness  $h_{\text{dep}}$ , sometimes expressed as a fraction of the stratum corneum thickness  $h_{\text{SC}}$ , i.e.  $f_{\text{dep}} = h_{\text{dep}} / h_{\text{SC}}$  (Kasting and Miller, 2006), plays an important role in the disposition of small doses of highly volatile compounds. The concept of a deposition region is based on the hypothesis that when a compound is applied to the skin surface in a liquid or semisolid formulation, it enters the desquamating SC layers by convection. These desquamating SC layers trap the compound and prevent it from rapidly evaporating, which in turn increases the available dose for permeation. The data in Table 2 and Fig. 1 are consistent with this hypothesis. Although absolute mass absorbed increases with increasing dose (Table 2), the percentage of dose absorbed decreases (Fig. 1). This reversal reflects the fact that, for large doses, much of the applied VOC resides above the SC. This material evaporates more rapidly than VOC trapped within the deposition region, although some of it is eventually absorbed as diffusion proceeds in the SC and lower skin layers. For smaller doses a larger percentage of the VOC is initially trapped in the deposition region, resulting in less evaporation and more diffusion into the lower layers of the SC.

It had seemed possible to us that the more aggressive VOCs (e.g. benzene, 1,2-DCE) might exhibit larger deposition regions than less aggressive or larger molecular weight permeants. This possibility is not ruled out by our analysis. However, after considerable variation of this parameter in the diffusion model (Gajjar, 2010), we concluded that a value of  $f_{\text{dep}} = 0.1$  provided the best fit to the VOC data when all four substances were considered. This finding is consistent with the original premise that approximately the upper 10% of the SC is undergoing desquamation (Kasting and Miller, 2006). Increasing the value of  $f_{\text{dep}}$  for benzene and 1,2-DCE led to only small improvement in the fits to these data. The more important factors were the diffusion and partition coefficients discussed below.

### Stratum corneum diffusion and partition coefficients

It may be seen from Fig. 2 that measured absorption profiles for all four VOCs tested departed from the a priori model predictions (dashed lines), with deviations increasing in the order ethanol < acetone < benzene < 1,2-DCE. This order accords qualitatively with the capacity of these solvents to dissolve or extract SC lipids. For ethanol, cumulative absorption (reflected by the AUC in Fig. 2a) was relatively well predicted, but substantial underpredictions occurred for the more aggressive solvents. The initial absorption rate was actually best estimated for acetone, but all four compounds showed more prolonged absorption profiles than those predicted from the a priori model. The discrepancies were improved but not eliminated by fitting the SC diffusion coefficient,  $D_{\text{SC}}$ , and SC/water partition coefficient,  $K_{\text{SC}}$ , to the cumulative absorption data (solid lines in Fig. 2). This procedure gave reasonable matches to the AUCs, but less satisfactory agreement with the absorption time course. The three more aggressive solvents still showed more prolonged absorption than can be accommodated by a Fickian diffusion model. This finding suggests that these compounds alter their own diffusivities and partition coefficients in the SC in a time-dependent manner. This inference is reinforced by comparison with the steady-state VOC absorption data in Frasch et al. (2007) as discussed below.

Frasch et al. (2007) conducted steady-state skin permeation experiments on three VOCs using large, occluded doses applied to hairless guinea pig (HGP) skin mounted in Franz diffusion cells. The compounds were applied neat in two different laboratories and as saturated aqueous solutions in the Frasch laboratory. We focus here on the results for 1,2-DCE, which are summarized in Table 4.

The experimental steady state flux for 1,2-DCE was 1000–6000  $\mu\text{g} \cdot \text{cm}^{-2} \text{h}^{-1}$ , depending on the laboratory and the dose solution. The flux estimated by the diffusion model was 25–80  $\mu\text{g} \cdot \text{cm}^{-2} \text{h}^{-1}$ , depending on the level of skin hydration chosen for the simulation. The discrepancy between the neat DCE results and the model prediction for partially hydrated skin was a factor of 150–250. To shed some light on this striking difference, we repeated the model calculations with the stratum corneum given the same diffusion and partition coefficients as the viable epidermis and dermis, and with the total skin thickness set equal to the value reported by Frasch (317  $\mu\text{m}$ ). Effectively, the stratum corneum was removed by this procedure, since it is much thinner than the other layers. The steady state flux for neat 1,2-DCE calculated according to this procedure was 3530  $\mu\text{g} \cdot \text{cm}^{-2} \text{h}^{-1}$ , a value very close to the experimental measurements in Table 4. The inference from this exercise is that prolonged exposure of HGP skin in vitro to neat 1,2-DCE effectively destroyed the lipid barrier in the stratum corneum, resulting in an absorption rate that was controlled primarily by the viable epidermis and dermis.

The finite dose skin permeation experiments in our laboratory (Figs. 1 and 2) led to much lower absorption rates than those in Frasch et al. (2007), yet the diffusion model calculations summarized in Table 3 and Fig. 2 imply that mild barrier disruption occurred even in these small, transient exposures. This result is important to bear in mind when conducting dermal risk assessments for aggressive VOCs.

### Opportunities for improvement in diffusion model

Our past research has shown the diffusion model can accurately estimate absorption of small doses of mild, moderately lipophilic compounds like benzyl alcohol (Miller et al., 2006) and DEET (Kasting et al., 2008a). Difficulties are encountered, however, with large or concentrated doses of compounds that can impact skin permeability including the pesticides parathion (Miller and Kasting, 2010) and tecnazene (Bhatt et al., 2008). The model underpredicts absorption in both of these cases. It is clear from the present study that VOCs are another chemical class for which accurate predictions are not yet possible. The comments below reflect our thinking as to where improvements are most needed.

**Evaporation mass transfer model.** The evaporation model employed in the present analysis was carefully calibrated for the in vitro Franz cell environment commonly employed in our laboratory (Gajjar et al., 2013). The fact that adjustments of the a priori value of the evaporation mass transfer coefficient  $k_{\text{evap}}$  of no greater than 13% (Table 3) were required to optimize the fit to the experimental data for the VOCs

**Table 4**

Comparison of steady-state flux values for 1,2-DCE in HGP skin (Frasch et al., 2007) to those calculated using the a priori diffusion model (Dancik et al., 2013).

Parameter	Neat	Aqueous
	Flux ( $\mu\text{g} \cdot \text{cm}^{-2} \text{h}^{-1}$ )	
Experimental steady-state flux (HFF) <sup>a</sup>	6280 $\pm$ 1380	1076 $\pm$ 178
Experimental steady-state flux (JNM) <sup>a</sup>	3842 $\pm$ 712	–
Diffusion model maximum flux <sup>b</sup>	25.2 <sup>c</sup>	79.8 <sup>d</sup>

<sup>a</sup> Frasch et al. (2007), Table 3.

<sup>b</sup> Values calculated using the Excel® spreadsheet version (Dancik et al., 2013). The flux value presently reported for aqueous solutions by the Web version (Fedorowicz et al., 2011) has a scaling error.

<sup>c</sup> A priori value calculated for partially hydrated skin.

<sup>d</sup> A priori value calculated for fully hydrated skin.



studied in this report attest to the accuracy of this model. However, the identification of the appropriate values (or ranges) of wind velocities for use with common human exposure scenarios has not been adequately addressed. The investigators wish to point out a recent development in this area that may be of value to risk assessors. Gong et al. have conducted a thorough analysis of the air/skin mass transfer coefficient for the *inverse* process of VOCs absorbing into the skin from the atmosphere under a variety of *in vivo* exposure conditions (Gong et al., 2014). They combined this analysis with an SC permeability model very similar to our own in order to predict dermal uptake of VOCs from contaminated air. Because skin evaporation and skin deposition of VOCs are inherently symmetrical processes, differing only in the direction of the VOC concentration gradient, it should be possible to apply Gong et al.'s analysis to evaporation of VOCs from the skin in the human exposure scenarios considered by these workers. We recommend this as an extension to the present model.

**Partition coefficients.** A significant source of error in the *a priori* model calculation could be the experimental data utilized to calibrate the underlying model for the stratum corneum/water partition coefficient. Experimental partition coefficients are obtained from dilute aqueous solution experiments that do not always predict the results of concentrated solutions applied to the skin. The data collected by Nitsche et al. (2006) showed a large variability for partition coefficients of highly lipophilic compounds. In addition, in our laboratory, we have found that large doses of concentrated pesticide solutions applied to the skin increase skin permeability relative to that observed at low doses (Bhatt et al., 2008; Miller and Kasting, 2010). These analyses suggested that the increase was largely associated with changes associated with the solute's partition coefficient in SC rather than the diffusion coefficient. There is evidence that this phenomenon occurs *in vivo* as well as *in vitro*, if the current model is applied to published dermal absorption data in humans, e.g. (Nolan et al., 1984). This complicates the interpretation of dose relationships for finite dose exposures as discussed recently by Frasch et al. (2014). It may be suggested that a correction factor ( $>10$ ) be applied for model predictions involving transient exposures of partially hydrated skin to neat or concentrated solvents.

**Stratum corneum solubility and swelling.** It is widely accepted that the ethanol–water cosolvent system is one of the most effective for producing substantial increases in permeation for a variety of compounds. In 1989, Berner et al. (1989a) published a thorough study detailing the uptake of ethanol and water per weight of dry SC from aqueous ethanol solutions at 32 °C. It is clear from the substantial amounts of both solvents absorbed that ethanol and water co-swell the skin. Based on this work, we initially estimated  $K_{sc}$  for ethanol in partially hydrated skin to be 0.39 as listed in Table 3 (Gajjar, 2010); this value was subsequently adjusted to 0.30 (Ray Chaudhuri et al., 2009). But, due to consistent underpredictions from the diffusion model similar to those described here, we later relaxed this limit and allowed ethanol and other organic compounds to partition into SC at even higher levels (Dancik et al., 2013). Partition coefficients of this magnitude or larger for water-miscible solutes can only be obtained through physical swelling of the substrate. The present diffusion model is parameterized for two hydration states corresponding to partial and full hydration of the SC (Dancik et al., 2013), but it does not allow the skin to transiently swell. For very soluble compounds like ethanol and acetone, this is a limitation that must be acknowledged.

More recently, Bunge et al. published thorough results detailing the permeation of 2-butoxyethanol (BE) and water in rat skin (Bunge et al., 2012). These workers demonstrated three distinct behavior profiles for BE flux with increasing weight fraction BE. When the weight fraction of BE was approximately less than 0.2, BE flux increased proportionally to its concentration. There was a relatively constant flux of BE at BE weight fractions of 0.2 to 0.8 and then a dramatic decrease in flux for BE weight

fraction greater than 0.8. They showed that the drastic drop in activity-normalized BE flux at high BE weight fraction coincided with a decrease in water activity from 0.9 at BE weight fraction 0.8 to zero for neat BE. These results demonstrated a reduced BE flux arising from skin dehydration.

Both abovementioned studies strongly suggest that a transient SC swelling model is required in order to quantitatively explain skin permeation results for concentrated solutions of small, water miscible solvents like ethanol and acetone. For small, lipophilic solvents like benzene and 1,2-DCE, our results suggest that a swelling model is also appropriate. We hypothesize that most of the swelling for ethanol involves the corneocyte phase of the SC, whereas that for benzene and 1,2-DCE involves primarily the intercellular lipids. Acetone may be a mixed case, as it is both water-miscible and a good solvent for SC lipids.

## Summary

This work demonstrates the multiple challenges in developing a comprehensive computational model for skin absorption, as simultaneous physical, chemical and biological processes influence absorption kinetics. Our main goal is to be able to confidently use the model to make predictions for drug delivery or risk assessment in multiple scenarios, such as splash exposure of a liquid in a factory setting or vapor-phase absorption in varying environments. As can be seen in this study, the present model is more accurate when dose amounts are small and disruption to the stratum corneum is less. A correction factor to the *a priori* model absorption predictions on the order of 10X is suggested for transient skin exposures to aggressive chemicals including acetone, benzene and 1,2-DCE. Continued focus on the mechanism of barrier disruption by VOCs and other organic chemicals will be useful in making more precise estimates of dermal exposure under varying conditions.

## Conflict of interest

The authors declare that there are no conflicts of interest.

## Acknowledgments

The authors acknowledge financial support from the National Institute for Occupational Safety & Health, Grant No. R01 OH007529. However, the views expressed here are those of the authors and have not been endorsed by NIOSH. We thank Matthew Miller for advice regarding the diffusion model calculations.

## References

- Abrams, K., Harvell, J.D., Shriner, D., Wertz, P., Maibach, H., Maibach, H.I., 1993. Effect of organic solvents on *in vitro* human skin water barrier function. *J. Invest. Dermatol.* 101, 609–613.
- Berner, B., Juang, R.-H., Mazzenga, G.C., 1989a. Ethanol and water sorption into stratum corneum and model systems. *J. Pharm. Sci.* 78, 472–476.
- Berner, B., Mazzenga, G.C., Otte, J.H., Steffens, R.J., Juang, R.-H., Ebert, C.D., 1989b. Ethanol: water mutually enhanced transdermal therapeutic system II: skin permeation of ethanol and nitroglycerin. *J. Pharm. Sci.* 78, 402–407.
- Bevington, P.R., 1969. *Data Reduction and Error Analysis for the Physical Sciences*. McGraw-Hill, New York.
- Bhatt, V.D., Soman, R.S., Miller, M.A., Kasting, G.B., 2008. Permeation of tecnazene through human skin *in vitro* as assessed by HS-SPME and GC-MS. *Environ. Sci. Technol.* 42, 6587–6592.
- Bommannan, D., Potts, R.O., Guy, R.H., 1991. Examination of the effect of ethanol on human stratum corneum *in vivo* using infrared spectroscopy. *J. Control. Release* 16, 299–304.
- Bunge, A.L., Persichetti, J.M., Payan, J.P., 2012. Explaining skin permeation of 2-butoxyethanol from neat and aqueous solutions. *Int. J. Pharm.* 435, 50–62.
- Campbell, P.S., Chandrasekaran, S.K., 1983. Dosage for commission drug and percutaneous absorption enhancer. ALZA Corporation, U.S. Patent 4379454.
- Cesarro, A.N., 1946. Is benzene absorption possible? *Med. Lav.* 46, 194–198.
- Conca, G.L., Maltagliati, A., 1955. Study of the percutaneous benzene absorption. *Med. Lav.* 46, 194–198.
- Dancik, Y., Miller, M.A., Jaworska, J., Kasting, G.B., 2013. Design and performance of a spreadsheet-based model for estimating bioavailability of chemicals from dermal exposure. *Adv. Drug Deliv. Rev.* 65, 221–236.



- Denda, M., Wood, L.C., Emami, S., Calhoun, C., Brown, B.E., Elias, P.M., Feingold, K.R., 1996. The epidermal hyperplasia associated with repeated barrier disruption by acetone treatment or tape stripping cannot be attributed to increased water loss. *Arch. Dermatol. Res.* 288, 230–238.
- Fatasch, M., 1997. Ultrastructure of epidermal barrier after irritation. *Microsc. Res. Tech.* 37, 193–199.
- Fedorowicz, A., Miller, M.A., Frasch, H.F., Kasting, G.B., 2011. Finite dose skin permeation calculator. NIOSH, <http://www.cdc.gov/niosh/topics/skin/finiteSkinPermCalc.html>.
- Franz, T.J., 1984. Percutaneous absorption of benzene. In: MacFaland, H.N., Holdsworth, C.E., MacGregor, J.A., Call, R.W., Kane, M.L. (Eds.), *Applied Toxicology of Petroleum Hydrocarbons*. Princeton Scientific Publishers, Inc, Princeton, pp. 61–70.
- Franz, T.J., Lehman, P.A., 1990. The use of water permeability as a means of validation for skin integrity in vitro percutaneous absorption studies. *J. Invest. Dermatol.* 94, 525.
- Frasch, H.F., Barbero, A.M., Alachkar, H., McDougal, J.N., 2007. Skin penetration and lag times of neat and aqueous diethyl phthalate, 1,2-dichloroethane and naphthalene. *Cutan. Ocul. Toxicol.* 26, 147–160.
- Frasch, H.F., Bunge, A.L., Chen, C.-P., Cherrie, J.W., Dotson, G.S., Kasting, G.B., Kissel, J.C., Sahmel, J., Semple, S., Wilkinson, S., 2014. Analysis of finite dose dermal absorption data: implications for dermal exposure assessment. *J. Expo. Sci. Environ. Epidemiol.* 65–73.
- Gajjar, R.M., 2010. Absorption and Evaporation of Volatile Solvents from the Skin Surface. Ph.D. thesis, Winkler College of Pharmacy, University of Cincinnati, Cincinnati, OH.
- Gajjar, R.M., Miller, M.A., Kasting, G.B., 2013. Evaporation of volatile organic compounds from human skin in vitro. *Ann. Occup. Hyg.* 57, 853–865.
- Gale, R.M., Berggen, R.G., 1987. Transdermal delivery system for delivering nitroglycerin at high transdermal fluxes. ALZA Corporation, U.S. Patent 4615699.
- Gale, R.M., Goetz, V., Lee, E.S., Taskovich, L.T., Yum, S.I., 1984. Transdermal administration of fentanyl and device therefor ALZA Corporation, U.S. Patent 4588580.
- Gong, M., Zhang, Y., Weschler, C.J., 2014. Predicting dermal absorption of gas-phase chemicals: transient model development, evaluation, and application. *Indoor Air* 24, 292–306.
- Good, W.R., Powers, M.S., Campbell, P.S., Schenkel, L., 1985. A new transdermal delivery system for estradiol. *J. Control. Release* 2, 89–97.
- Gummer, C.L., Maibach, H.I., 1986. The penetration of [ $^{14}\text{C}$ ] ethanol and [ $^{14}\text{C}$ ] methanol through excised guinea-pig skin. *Food Chem. Toxicol.* 24, 305–309.
- Hanke, J., Dukiewicz, T., Piotrowski, J., 1961. Absorption of benzene through the skin in man. *Med. Pr.* 12, 413–426.
- Kasting, G.B., Bowman, L.A., 1990. DC electrical properties of frozen, excised human skin. *Pharm. Res.* 7, 134–143.
- Kasting, G.B., Miller, M.A., 2006. Kinetics of finite dose absorption through skin 2. Volatile compounds. *J. Pharm. Sci.* 95, 268–280.
- Kasting, G.B., Filloon, T.G., Francis, W.R., Meredith, M.P., 1994. Improving the sensitivity of in vitro skin penetration experiments. *Pharm. Res.* 11, 1747–1754.
- Kasting, G.B., Miller, M.A., Bhatt, V., 2008a. A spreadsheet-based method for estimating the skin disposition of volatile compounds: application to N, N-diethyl-m-toluamide (DEET). *J. Occup. Environ. Hyg.* 10, 633–644.
- Kasting, G.B., Miller, M.A., Nitsche, J.M., 2008b. Absorption and evaporation of volatile compounds applied to skin. In: Walters, K.A., Roberts, M.S. (Eds.), *Dermatologic, Cosmeceutic and Cosmetic Development*. Informa Healthcare USA, New York, pp. 385–400.
- Laserew, N.V., Brussilowskaja, A.J., Lavroff, I.N., Lifschitz, F.B., 1931. On the permeability of the skin to benzene and benzene. *Arch. Hyg. Bakteriol.* 106, 112–122.
- Lodén, M., 1986. The in vitro permeability of human skin to benzene, ethylene glycol, formaldehyde, and n-hexane. *Acta Pharmacol. Toxicol.* 58, 382–389.
- Maibach, H.I., Anjo, D.M., 1981. Percutaneous penetration of benzene and benzene contained in solvents used in the rubber industry. *Arch. Environ. Health* 36, 256–260.
- Man, M.-Q., Feingold, K.R., Elias, P.M., 1993. Exogenous lipids influence permeability barrier recovery in acetone-treated murine skin. *Arch. Dermatol.* 129, 728–738.
- Miller, M.A., Kasting, G.B., 2010. Towards a better understanding of pesticide dermal absorption: diffusion model analysis of parathion absorption in vitro and in vivo. *J. Toxicol. Environ. Health A* 73, 284–300.
- Miller, M.A., Bhatt, V., Kasting, G.B., 2006. Absorption and evaporation of benzyl alcohol from skin. *J. Pharm. Sci.* 95, 281–291.
- Morgan, D.L., Cooper, S.W., Carlock, D.L., Sykora, J.J., Sutton, B., Mattie, D.R., McDougal, J.N., 1991. Dermal absorption of neat and aqueous volatile organic chemicals in the Fischer 344 rat. *Environ. Res.* 55, 51–63.
- Nitsche, J.M., Kasting, G.B., 2008. Biophysical models for skin transport and absorption. In: Roberts, M.S., Walters, K.A. (Eds.), *Dermal Absorption and Toxicity Assessment*. Informa Healthcare USA, New York, pp. 249–267.
- Nitsche, J.M., Wang, T.-F., Kasting, G.B., 2006. A two-phase analysis of solute partitioning into the stratum corneum. *J. Pharm. Sci.* 95, 649–666.
- Nolan, R.J., Rick, D.L., Freshour, M.L., Saunders, J.H., 1984. Chlorpyrifos: pharmacokinetics in human volunteers. *Toxicol. Appl. Pharmacol.* 73, 8–15.
- Pendlington, R.U., Whittle, E., Robinson, J.A., Howes, D., 2001. Fate of ethanol topically applied to skin. *Food Chem. Toxicol.* 39, 169–174.
- Ray Chaudhuri, S., Gajjar, R.M., Krantz, W.B., Kasting, G.B., 2009. Percutaneous absorption of volatile solvents following transient liquid exposures. II. Ethanol. *Chem. Eng. Sci.* 64, 1665–1672.
- Santhanam, A., Miller, M.A., Kasting, G.B., 2005. Absorption and evaporation of N, N-diethyl-m-toluamide (DEET) from human skin in vitro. *Toxicol. Appl. Pharmacol.* 204, 81–90.
- Scheuplein, R.J., Blank, I.H., 1973. Mechanism of percutaneous absorption. IV. Penetration of nonelectrolyte (alcohols) from aqueous solutions and from pure liquids. *J. Invest. Dermatol.* 60, 286–296.
- Susten, A.S., Dames, B.L., Burg, J.R., Niemeier, R.W., 1985. Percutaneous penetration of benzene in hairless mice: an estimate of dermal absorption during tire-building operations. *Am. J. Ind. Med.* 7, 323–335.
- Tsuruta, H., 1975. Percutaneous absorption of organic solvents 1) comparative study of the in vivo percutaneous absorption of chlorinated solvents in mice. *Ind. Health* 13, 227–236.
- Tsuruta, H., 1977. Percutaneous absorption of organic solvents 2) a method for measuring the penetration rate of chlorinated solvents through excised rat skin. *Ind. Health* 15, 131–139.
- Tsuruta, H., 1982. Percutaneous absorption of organic solvents. III. On the penetration rates of hydrophobic solvents through the excised rat skin. *Ind. Health* 20, 335–345.
- Tsuruta, H., 1989. Skin absorption of organic solvent vapors in nude mice in vivo. *Ind. Health* 27, 37–47.
- US\_EPA, 2009a. Benzene. <http://www.epa.gov/ttn/atw/hlthef/benzene.html>.
- US\_EPA, 2009b. Estimation Programs Interface Suite™ for Microsoft® Windows. United States Environmental Protection Agency, Washington, DC, USA.
- US\_EPA, 2009c. Ethylene Dichloride (1,2-Dichloroethane). <http://www.epa.gov/airtoxics/hlthef/di-ethan.html>.
- Williams, P.L., Brooks, J.D., O, I.A., Monteiro-Riviere, N.A., Riviere, J.E., 1994. Determination of physicochemical properties of phenol, p-nitrophenol, acetone and ethanol relevant to quantitating their percutaneous absorption in porcine skin. *Res. Commun. Chem. Pathol. Pharmacol.* 83, 61–75.
- Williams, P.R.D., Sahmel, J., Knutsen, J., Spencer, J., Bunge, A.L., 2011. Dermal absorption of benzene in occupational settings: estimating flux and applications for risk assessment. *Crit. Rev. Toxicol.* 41, 111–142.